



## Open Archive TOULOUSE Archive Ouverte (OATAO)

OATAO is an open access repository that collects the work of Toulouse researchers and makes it freely available over the web where possible.

This is an author-deposited version published in : <http://oatao.univ-toulouse.fr/>  
Eprints ID : 20137

**To link to this article** : DOI: 10.1063/1.5024346

URL : <http://doi.org/10.1063/1.5024346>

**To cite this version** : Ncube, Siphephile and Coleman, Chistopher and de Sousa, Alvaro S. and Nie, Chunyang and Lonchambon, Pierre and Flahaut, Emmanuel and Strydom, Andrew and Bhattacharyya, Somnath *Observation of strong Kondo like features and co-tunnelling in superparamagnetic GdCl<sub>3</sub> filled 1D nanomagnets*. (2018) Journal of Applied Physics, vol. 123 (n° 21). pp. 213901/1-213901/7. ISSN 0021-8979

Any correspondence concerning this service should be sent to the repository administrator: [staff-oatao@listes-diff.inp-toulouse.fr](mailto:staff-oatao@listes-diff.inp-toulouse.fr)

# Observation of strong Kondo like features and co-tunnelling in superparamagnetic GdCl<sub>3</sub> filled 1D nanomagnets

S. Ncube,<sup>1</sup> C. Coleman,<sup>1</sup> A. S. de Sousa,<sup>2</sup> C. Nie,<sup>3</sup> P. Lonchambon,<sup>3</sup> E. Flahaut,<sup>3</sup> A. Strydom,<sup>4,5</sup> and S. Bhattacharyya<sup>1,a)</sup>

<sup>1</sup>Nano Scale Transport Physics Laboratory, School of Physics, and DST/NRF Centre of Excellence in Strong Materials, University of the Witwatersrand, Johannesburg, South Africa

<sup>2</sup>School of Chemistry, University of the Witwatersrand, Johannesburg, South Africa

<sup>3</sup>CIRIMAT, Université de Toulouse, CNRS, INPT, UPS, UMR CNRS UPS INP N°5085, Université Toulouse Paul Sabatier, Bât. CIRIMAT, 118, route de Narbonne, 31062 Toulouse cedex 9, France

<sup>4</sup>Highly Correlated Matter Research Group, Department of Physics, University of Johannesburg, Auckland Park 2006, South Africa

<sup>5</sup>Max Planck Institute for Chemical Physics of Solids, Nothnitzer str. 40, D 01187 Dresden, Germany

Filling of carbon nanotubes has been tailored over years to modify the exceptional properties of the 1 dimensional conductor for magnetic property based applications. Hence, such a system exploits the spin and charge property of the electron, analogous to a quantum conductor coupled to magnetic impurities, which poses an interesting scenario for the study of Kondo physics and related phenomena. We report on the electronic transport properties of MWNTs filled with GdCl<sub>3</sub> nanomagnets, which clearly show the co existence of Kondo correlation and cotunnelling within the superparamagnetic limit. The Fermi liquid description of the Kondo effect and the interpolation scheme are fitted to the resistance temperature dependence yielding the onset of the Kondo scattering temperature and a Kondo temperature for this nanocomposite, respectively. Cotunnelling of conduction electrons interfering with a Kondo type interaction has been verified from the exponential decay of the intensity of the fano shaped nonzero bias anomalous conductance peaks, which also show strong resonant features observed only in GdCl<sub>3</sub> filled MWNT devices. Hence, these features are explained in terms of magnetic coherence and spin flip effects along with the competition between the Kondo effect and co tunneling. This study raises a new possibility of tailoring magnetic interactions for spintronic applications in carbon nanotube systems.

<https://doi.org/10.1063/1.5024346>

## I. INTRODUCTION

Numerous efforts have been made to investigate the competition between the many body Kondo effect and other co existing phenomena like cotunnelling, Ruderman Kittel Kasuya Yosida (RKKY) interaction, and superconductivity<sup>1-4</sup> in strongly interacting correlated electron systems. The co existence of these phenomena gives rise to new device functionalities and a prospect to explore the atypical physics.<sup>5-8</sup> A system which possesses quantum transport properties, while being ferromagnetic and semiconducting can be explored for spintronic applications. Modified carbon nanotubes (CNTs) are ideal platforms for this study as they have already been extensively researched as quantum dots for quantum computing and spintronic applications.<sup>9-11</sup> The exceptional properties of carbon have allowed for the modification and tailoring of CNT properties by attaching desired supramolecular complexes<sup>12,13</sup> and filling with nanomagnets.<sup>14</sup> Conventional spintronic devices are fabricated using such modified or with pristine CNTs contacted to ferromagnetic leads.<sup>13,15,16</sup> There is however another modification route that has to date not been thoroughly investigated for spintronic applications: filling of MWNTs with magnetic

materials. Filling of CNTs with ferromagnetic materials has been attempted over a long period of time in order to improve their electronic and magnetic properties for multifunctional applications ranging from data storage to bio electronics. For nanoelectronic applications, filling has been largely unsuccessful due to the lack of observation of the many body effects like Kondo, which is directly related to the quantum nature of the electron, and cotunnelling effects. However, a significant deviation of this trend from a conventional Kondo physics of a pure ferromagnetic material with equally spaced magnetic impurities has been noticed. Filling of MWNTs has been shown to preserve the magnetic nanoparticles from oxidation; hence, the magnetic properties are retained ensuring long term stability. It has been shown that upon modification with magnetic materials, the magnetotransport properties of CNT are considerably affected and become sensitive to the magnetic state of the modifying elements.<sup>17</sup> Due to their low dimensional nature and high aspect ratio, the combination of CNTs and magnetic entities can give rise to exotic features like the Kondo effect,<sup>4</sup> a many body phenomenon which is known to arise when a localized magnetic impurity interacts with the spin of the conduction electrons of a nonmagnetic metallic host. In this work, we focus on the study of devices fabricated from bundles of GdCl<sub>3</sub> filled MWNTs (GdCl<sub>3</sub>@MWNT). At the nanoscale, the Kondo effect has

<sup>a)</sup>E mail: Somnath.Bhattacharyya@wits.ac.za

been observed in individual CNTs, quantum dots, individual molecules, and quantum point contacts by direct probing of the local density of states using scanning tunnelling microscopy (STM).<sup>18–21</sup> SWNTs decorated with cobalt nanoclusters exhibit Kondo resonances observed as a narrow peak near the Fermi level.<sup>22</sup> In this work, we show the emergence of Kondo like resonances in the conductance and cotunnelling effects in devices fabricated from a network of gadolinium chloride filled MWNTs. This is explained by the device architecture employed and multichannel effect dominant in bundles. The  $\text{GdCl}_3$ @MWNTs exhibit a superparamagnetic transition at low temperatures, and a cotunnelling to Kondo effect dominated electronic transport, which can be related to the blocking temperature.

## II. METHODOLOGY

**Synthesis:** MWNTs used were synthesized by Catalytic Chemical Vapour Deposition using a Co:Mo MgO catalyst with an elemental composition of  $\text{Mg}_{0.9}\text{Co}_{0.033}\text{Mo}_{0.067}\text{O}$ . The catalyst was heated in an atmosphere containing 36% of  $\text{CH}_4$  and 64% of  $\text{H}_2$ , at a total flow rate of 15L/h, starting from room temperature to 1000 °C at 5°/min. No dwell was applied, and the gaseous atmosphere was maintained constant during all the procedures. The nanocomposite powder obtained was processed with a concentrated aqueous solution of HCl in order to dissolve all the accessible catalyst. After thoroughly washing with deionised water on a filtration setup (PP membrane, 0.45  $\mu\text{m}$  pore size), the sample was freeze dried.

### A. Modification

**Filling MWNTs with  $\text{GdCl}_3$ :** 5 g of  $\text{GdCl}_3$  anhydrous powder (purity 99.99%, Sigma Aldrich) were mixed together with 180 mg of dry CNTs using a mortar and pestle in a glove tent flushed with dry nitrogen. The mixture was

transferred into a quartz ampoule. The ampoule was connected to a vacuum line and sealed. The sealed ampoule was transferred into a tubular furnace and submitted to the following heat treatment: heating from room temperature to 630 °C at 5°/min. A dwell of 24 h was applied, after which the sample was first cooled down very slowly from 630 °C to 580 °C at 0.1 °C/min, to 480 °C at 1 °C/min, and finally to room temperature at 5 °C/min. The ampoule was cut using a glass knife and the sample recovered. It was washed with deionised water and then with concentrated HCl [6 mol/L] in order to dissolve gadolinium oxide which forms spontaneously during the washing with water. Finally, the sample was freeze dried.

**Structural characterization:** HRTEM of the  $\text{GdCl}_3$ @MWNTs (Fig. 1) reveals the presence of discontinuous rod like nanostructures in the core of the innermost tube with an approximate length of 10–30 nm. This technique for filling MWNTs has been investigated before, and HRTEM studies have confirmed the filled material as  $\text{GdCl}_3$  through investigations of the crystal lattice structure.<sup>23</sup> Quantification of the  $\text{Gd}^{3+}$  concentration was done by a microwave assisted  $\text{HNO}_3$  digestion (Ultra Wave Milestone) and analysis by ICP AES (ICAP 6500 Thermofisher Scientific). It was found that  $\text{GdCl}_3$ @MWNTs contain approximately 0.26 wt. % cobalt with a concentration of 1.08% gadolinium. Pristine MWNTs from the synthesis mentioned earlier were also analyzed and contained Co: 0.54 and Mo: 1.66 wt. %. This was measured to establish the concentration of catalyst impurities before filling. From the Raman data [Fig. 1(b)], we use the Tuinstra Koenig equation<sup>24</sup> to find a crystallite size of 13.33 nm. An upward shift of the Raman G peak position is observed when compared to the pristine MWNTs (1582  $\text{cm}^{-1}$ ) of 5  $\text{cm}^{-1}$  which is similar to what has been reported for SWNT filled with  $\text{CoBr}_2$ ;<sup>25,26</sup> hence, the shift in G peak was believed to be a result of  $\text{Gd}^{3+}$  doping. Upon deconvolution, it was

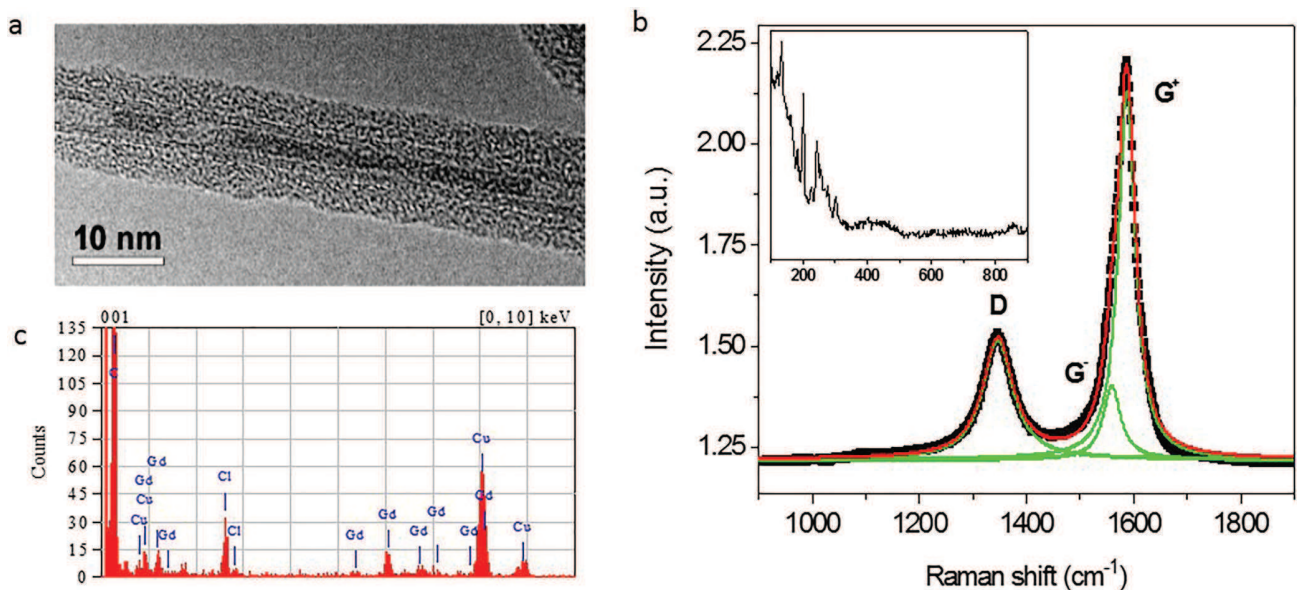


FIG. 1. (a) HRTEM image of  $\text{GdCl}_3$ @MWNTs showing rod like structures inside the innermost tube; (b) the Raman spectrum of the  $\text{GdCl}_3$ @MWNT, as can be seen the samples exhibits spectrum for low disordered CNT with pronounced G band and small  $I_D/I_G$  ratio. Convolution shows the G band can be split into two sub peaks. Inset shows multiple low wave number peak uncharacteristic of pristine MWNT. (c) EDX analysis corresponding to the boxed area in the HRTEM image showing the presence of Gd and Cl in the sample.

established that the G peak could be split into two components identified as  $G^+$  and  $G^-$  which correspond to vibrational modes along nanotube axis and around circumferential direction, respectively. The increased width of the Raman G and D peaks was taken as an indication of increased disorder.<sup>14</sup> In addition to the expected D and G band, the Raman spectra of the filled CNTs exhibit multiple small sharp peaks at low Raman wavenumbers, which have been observed in SWNTs, DWNTs,<sup>27</sup> and MWNTs prepared using arc discharge synthesis route,<sup>28</sup> but they have not been observed in CVD synthesized MWNTs. These peaks are generally attributed to the radial breathing modes (RBM) of CNTs. The observation of peaks in the range of 50–200  $\text{cm}^{-1}$  may however also be related to the four vibrational modes of  $\text{GdCl}_3$ , which are expected to occur at 93, 185, 199, and 230  $\text{cm}^{-1}$  which have been observed for other lanthanide trichloride samples.<sup>29–32</sup>

Both Gd and Cl are found simultaneously by EDX analysis as shown in Fig. 1(c).  $\text{GdCl}_3$  is perfectly stable in the filling conditions (no reactivity with carbon even at its melting point), so starting with MWNTs and  $\text{GdCl}_3$  can only lead to MWNTs and  $\text{GdCl}_3$  after filling. Some  $\text{Gd}_2\text{O}_3$  may be formed during the dissolution of  $\text{GdCl}_3$  if the pH is not acidic enough. This is the reason that the excess of  $\text{GdCl}_3$  after filling is washed using an aqueous solution of HCl.

### III. RESULTS AND DISCUSSION

#### A. Magnetic property studies

The Gd filled sample showed no magnetic remanence or coercive field [Fig. 2(a)]. From literature, Gd incorporated carbon nanotubes filled or functionalization exhibit superparamagnetism.<sup>33,34</sup> The hallmark of this effect is the bifurcation observed between field cooled (FC) and zero field cooled (ZFC) susceptibility, as shown in Fig. 2(b). This is observed only in the filled CNTs indicating the non interaction of magnetic centres leading to superparamagnetism. The bifurcation starts approximately at 100 K and upon decreasing the

temperature the gap broadens to 30 K where a sudden downward turn is observed in the FC data. We have thus identified two significant temperatures: the higher one is the bifurcation temperature and signifies the onset of the superparamagnetic phase, and the second lower temperature is the blocking temperature. The broad transition is a result of inhomogeneity in the magnetic particle size and corresponds to different size particles having a range of blocking temperatures. The inverse of the ZFC susceptibility was plotted as a function of temperature to determine the coupling mechanism.  $\text{GdCl}_3$ @MWNTs showed linearity down to near the determined blocking temperature and then decreases steeply. This is an indication of a phase transition. By using the Curie Weiss law (fitted to the linear part of the data), a negative Weiss constant of 55 K was obtained, indicating antiferromagnetic exchange interaction. Antiferromagnetic exchange requires the existence of interaction between two spin sublattices of different spin orientation. In the system studied here, the antiferromagnetic features are most likely due to the exchange between neighboring clusters of  $\text{GdCl}_3$  inter particle dominating over intra particle interactions. The delocalized electrons of the nanotubes are likely candidates for mediating the antiferromagnetism via the RKKY interaction. There is a screening effect from outer walls which lowers the effective spin electron interaction. This along with the fewer mediating conduction electrons is likely to be the cause of the Weiss temperature observed in  $\text{GdCl}_3$ @MWNTs. Figure 2(b) shows the molar susceptibility plots used to determine the Weiss temperature and Curie constant, when calculating the effective moment in terms of the molar concentration of the Gd, which is determined from the elemental analysis. We calculate an effective moment and  $20.7 \mu_B$ . The large value reported here is a clear indication of interactions between the  $\text{GdCl}_3$  and electronic environment of the MWNTs. A control study of pristine MWNTs was conducted in order to establish any contribution resulting from catalyst impurities such as the Co, which was determined to be present from the elemental analysis. Although the control does show a slight paramagnetic

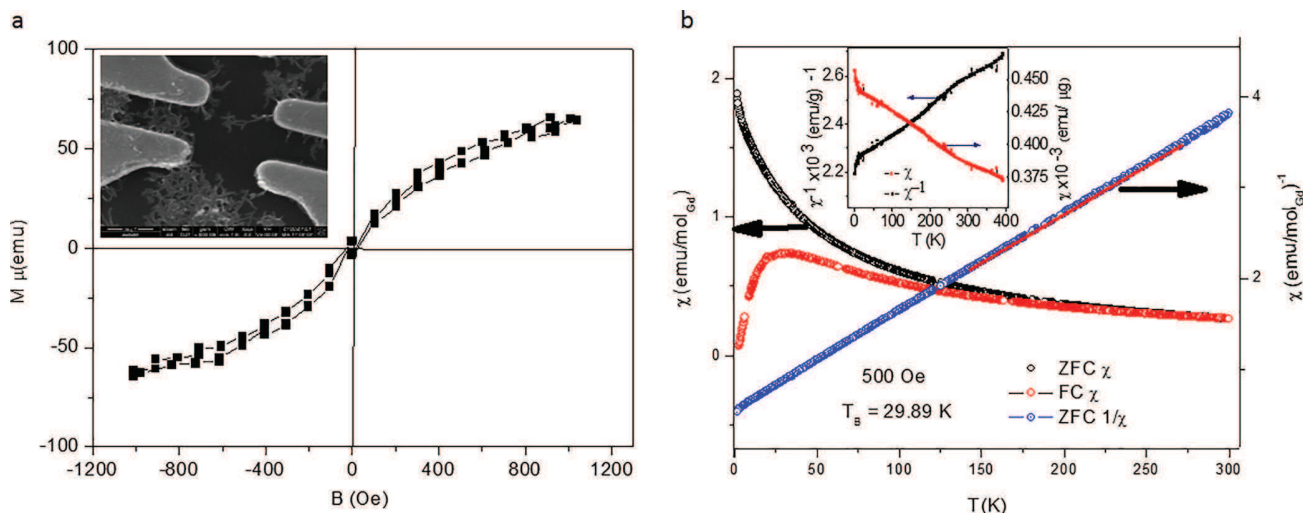


FIG. 2. (a) Hysteresis for the filled MWNT sample showing paramagnetic behaviour. Inset shows devices fabricated from  $\text{GdCl}_3$ @MWNTs. (b) Susceptibility and its inverse for the filled sample. As can be seen there is a clear bifurcation in FC and ZFC sweeps indicating superparamagnetism with a blocking temperature of 30 K. Inset shows susceptibility and inverse susceptibility of the pristine MWNTs.



signature, the response is orders of magnitude weaker than the response of the modified MWNTs [Fig. 2(b) inset] indicating that the dominant magnetic effects are a result of the filling of gadolinium species and not from catalyst impurities.

## B. Electronic transport

The increase in resistance as temperature decreases to 50 K has been analysed in light of Kondo scattering utilising the Fermi liquid description,<sup>35–37</sup> which has recently been successfully used for graphene devices

$$\rho(T) = \rho_{c1} + \rho_0 \left(1 - \left(\frac{T}{T_K}\right)^2\right), \quad (1)$$

$$\rho(T) = \rho_{c2} + \frac{\rho_0}{2} \left(1 - 0.47 \ln\left(\frac{1.2T}{T_K}\right)\right). \quad (2)$$

Equation (1) is valid for temperatures between resistance maxima up to approximately 150 K, where there is a change in transport mechanism that is described in Equation (2), as shown in Fig. 3(a). Both equations give a best fit to the data with a Kondo temperature of 137 K. The values of  $\rho_{c1}$  and  $\rho_{c2}$  have a discrepancy of within 12%, indicating reasonable self consistency between the two equations. This model does not however explain the additional turning point in the resistance temperature curve indicating that additional mechanisms at play. Thus, the Kondo temperature determined above ( $T_K$ ) is considered to be the temperature where Kondo scattering becomes significant (related to the bifurcation temperature observed in the susceptibility) or the onset Kondo temperature. The functional change in temperature dependence can also be related to a crossover in incoherent ( $\log T$  dependence) to coherent scattering regime ( $T^2$ ), which is sometimes observed in simple metallic systems due to phase translational invariance. One of the key concepts in this phase translational invariance is the formation of triplet states through to the Kondo effect, the excitation from a

singlet ground state to triplet state via the Kondo effects is well documented in carbon nanotube devices.<sup>38</sup> To establish the nature of decreasing low temperature resistance, the conductivity data are analysed in light of interpolation scheme taking into account competition between the Kondo effect and co tunnelling which is schematically shown in Fig. 4,<sup>3</sup> which has been successfully used to describe magnetic tunnel junctions with superparamagnetic particles embedded within the dielectric layer. As seen in Fig. 3(b), the red curve is a combination of the two interpolation formula used to indicate the cross over from a co tunnelling dominated to Kondo dominated regime given by

$$\sigma = a\sigma_D + b(\sigma_E + \sigma_K) \quad \text{with } a + b = 1. \quad (3)$$

Here,  $\sigma_D$  is the direct tunnelling conductivity between the electrodes and has previously been neglected when using this model. In order for a more realistic fit, we have however related  $\sigma_D$  to a conductance offset determined from the fitting to be  $\sigma_D = 6.6 \times 10^{-6} \mu\text{S}$ ; this effectively sets the coefficients  $a$  and  $b$  as 0.75 and 0.25, respectively.  $\sigma_K$  represents the conductivity term involving the Kondo effect and  $\sigma_E$  is the elastic conductivity not including spin flip events. According to Ref. 39, the conductivity term associated with the Kondo effect takes the form

$$\sigma_K = \sigma_0 \frac{T_{K2}^2}{T^2 + T_{K2}^2} \Big)^S, \quad (4)$$

$$\text{where } T_{K2}^2 = \frac{T_K}{\sqrt{2^{1/S} - 1}}. \quad (5)$$

As usual,  $S \sim 0.2$  and  $\sigma_0$  is related to the occupancy of electron clusters near the magnetic particles within the tubes; for perfectly symmetric barriers, it will have a value of  $\sigma_0 \leq (2e^2)/h$ . For these devices, we obtain a value of approximately  $7 \times 10^{-9}$  well within the expected range demonstrated by other magnetic tunnel junction devices. The

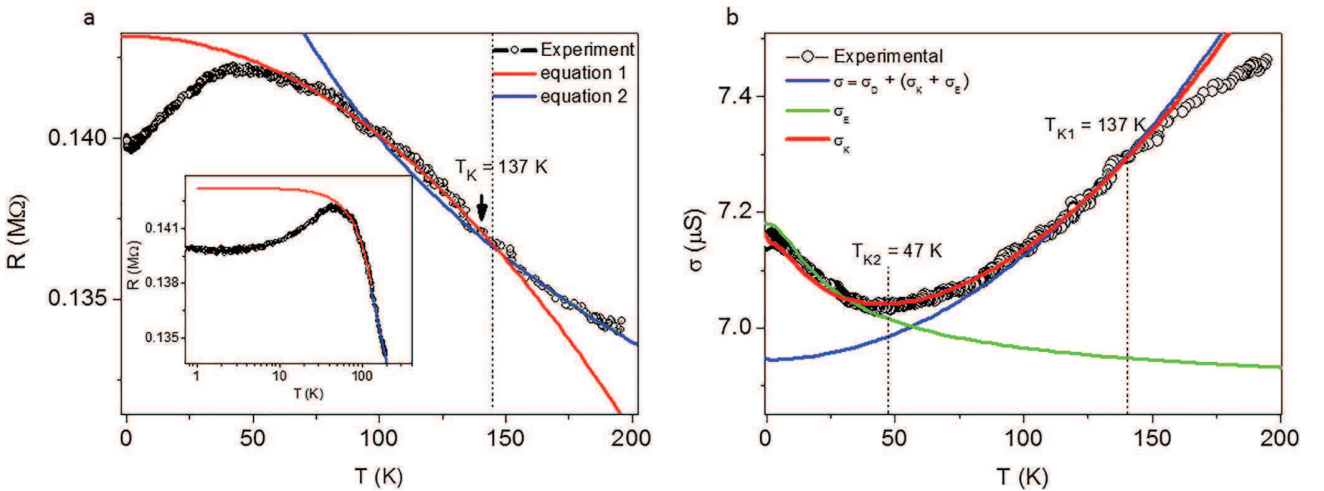


FIG. 3. The resistance as a function of temperature. (a) The red and blue lines are a fit to Eqs. (1) and (2), which yields a Kondo temperature of 137 K. The inset shows the same data plotted on a  $\log T$  scale to highlight the various transport crossover regimes. (b) The conductance as a function of temperature for the  $\text{GdCl}_3$ @MWNT sample. Here, the conductance shows a minimum at around 40 K and then increases sharply to saturation at 10 K. The fitted curve is the interpolation formula given by Eq. (3).

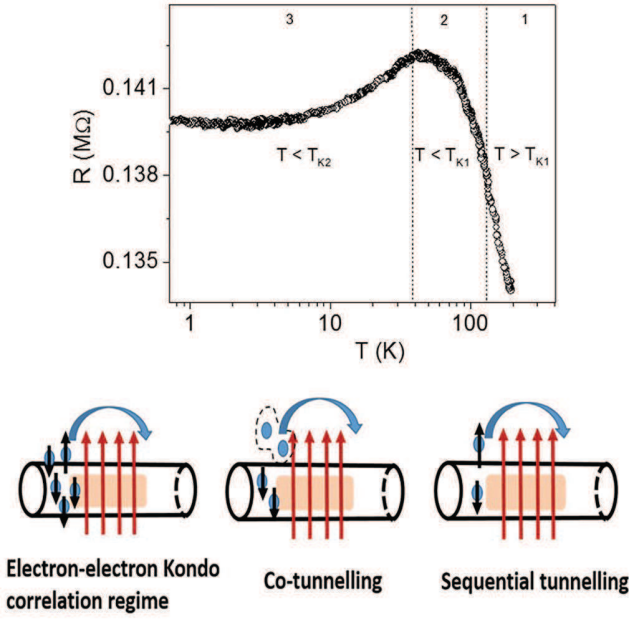
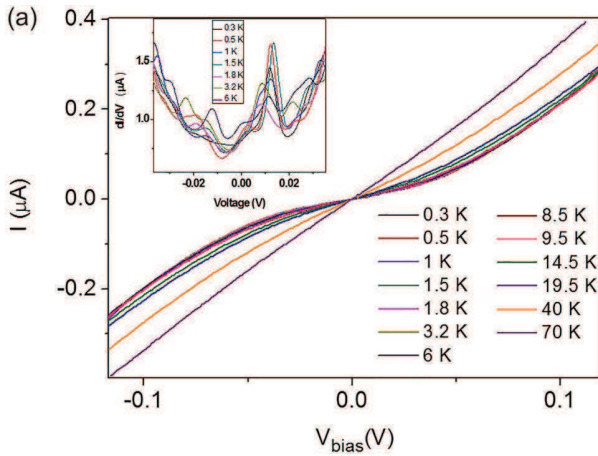


FIG. 4. A schematic showing the possible mechanisms for the changes observed in the temperature dependent resistance which is separated into three temperature regimes.  $T_{K1}$  as determined from the fitting given in Figs. 3(a) and 3(b) as well as the onset blocking temperature observed in the susceptibility indicates the Kondo spin flip event between  $\text{GdCl}_3$  and electrons. At a lower temperature, it is possible to have co tunneling events which occur through the formation of virtual states, such as the singlet pairing quasiparticle. As the switching of the nanoparticles decreases at lower temperatures, we reach a stage of maximum spin coherence and thus spin accumulation of electrons, and this regime is dominated by electron electron interactions, whereby the Kondo effect allows the correct spin polarization for tunneling to occur also observed as the sharp downturn in susceptibility.

elastic conductivity is given by a combination of sequential and co tunneling conductance terms, which take the form

$$\sigma_{cot} = \frac{2h}{3e^2} \frac{1}{R_T^2} \left( \frac{k_B T}{E_C} \right)^2; \quad (6a)$$

$$\sigma_{seq} = \frac{1}{2R_T^2} \left( 1 + \frac{E_C}{k_B T} \right)^{-1}. \quad (6b)$$



Here,  $R_T$  is the tunnelling resistance between electrodes and CNT bundles, and this quantity is determined from Equation (6b) to be  $R_T = 5.3 \text{ k}\Omega$ , which is slightly higher but of the same order magnitude as what has been reported for double magnetic tunnel junctions with embedded superparamagnetic NiFe nanoparticles.<sup>39</sup>  $E_C$  is the charging energy which is related to the size and shape and hence the capacitance of the magnetic nanoparticles and can, as a first approximation, be expressed as  $E_C = 2\pi\epsilon\epsilon_0 d$ , where  $\epsilon$  is the relative permittivity of the tunnelling barriers and  $d$  is the diameter of the nanoparticle rod. The Kondo temperature from this fitting is 47 K, which is in agreement with the point of inflection in the conductivity temperature curve. Thus, the  $R T$  behaviour is explained as a competition between tunneling events and the strengthening of the Kondo effect as temperature is lowered; at some point, the Kondo effect dominates over the tunnelling (47 K) and an inflection is observed. In order to verify the coexistence of co tunneling conductivity in the system, an analysis of the current voltage characteristics is undertaken as shown in Figs. 5(a) and 5(b). The slope of the  $I V$  sweeps change markedly upon lowering temperature, and we observe the formation of a gap (strong deviation from linearity) at a temperature below 40 K. As shown in the inset of Fig. 6(a), the differential conductance exhibits resonance peak features which are strongly temperature dependent. In order to probe the interaction of sequential and co tunneling conductivity, we rely on the theory developed for Coulomb gap inelastic co tunneling<sup>40,41</sup>

$$I(V) = \left( \frac{\hbar}{3\pi e^2 R_T^2 E_C^2} \right) \left[ (2\pi k_B T)^2 V + e^2 V^3 \right], \quad (7)$$

which describes the current as a sum of two terms, one linear and the other cubic in voltage. We thus fit the  $I V$  curves at different temperatures to the phenomenological expression

$$I(V) = AV + BV^3. \quad (8)$$

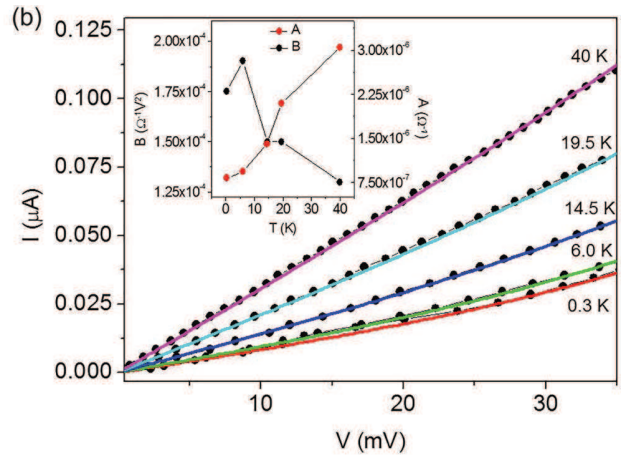


FIG. 5. (a) The current voltage characteristics of the  $\text{GdCl}_3/\text{MWNT}$  bundle device. There is a clear band gap opening at temperatures below 40 K compared to linear behaviour above that. Differential conductance (inset) shows the formation of temperature dependent resonance peaks. (b) The current voltage plots fit to Eqs. (6a) and (6b). The inset shows the evolution of the coefficients with increasing temperature.

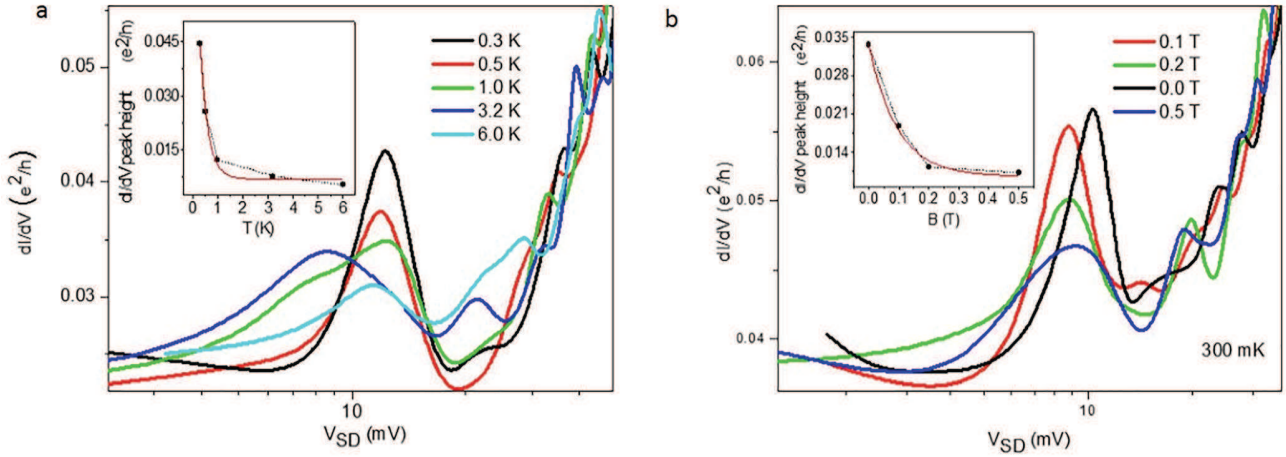


FIG. 6. (a) Temperature dependence of the differential conductance. The peak heights decrease exponentially as temperature increases, and we observe co tunneling step features and spectral shift as temperature increases. This is most likely due to crossover between sequential and co tunneling regimes. (b) Magnetic field dependence of the  $dI/dV$  peaks; magnetic field is seen to exponentially suppress the peak intensity.

Here, the ratio between the coefficients A and B are related to the strength of contribution, either sequential or co tunneling, to the current. The fit is shown in Fig. 5(b), and the trend of the coefficients A and B are shown in the inset as a function of temperature, and as can be seen, there the range of increase in coefficient A is seen to increase at a faster rate than the change in coefficient B; this was taken to explain the dominance of co tunneling over sequential tunnelling in this low current regime.<sup>40</sup> As mentioned previously, the differential conductance sweeps exhibit strong resonance peaks at around 10 mV. These peaks are temperature and magnetic field dependent and exponentially decrease in height with an increase in either parameter [shown in Figs. 6(a) and 6(b)]. Upon examining the temperature dependent  $dI/dV$ , we observe an apparent shifting and broadening of the peaks. These features can be related back to the competition between co tunneling and the Kondo effect. As the temperature is increased, the Kondo effect is suppressed and co tunneling is favoured, analogous to the conductance vs. temperature; this leads to the formation of co tunneling peaks at a slightly lower voltage indicated as a shoulder and eventual spectral shift of the Kondo peak. Similar features are observed in the B dependence. Following conventional analysis, the Kondo temperature can be extracted from these resonance peaks by examining the FWHM. In this case, the 300 mK zero field resonance peak gives a Kondo temperature of 40 K. This value is in excellent agreement with the value obtained from the conductivity fitting and is a significant temperature point as indicated by the susceptibility blocking temperature indicating that spin coherence becomes important for electron correlations.

#### IV. CONCLUSION

We have demonstrated the modification of magnetic and electronic properties of MWNTs filled with gadolinium chloride. The  $\text{GdCl}_3$ @MWNTs show signatures of superparamagnetism in the susceptibility measurements with a broad transition from superparamagnetic to blocked state due to

the different particle sizes of the nanorods. Transport measurements were conducted on bundle CNT devices, which showed interesting electron spin correlations around and below the blocking temperature. We have analyzed the transport considering a competition between the Kondo effect and co tunneling following what has been reported for double magnetic tunnel junctions. We observe non zero resonance peaks in the differential conductance, which indicate the dominance of the Kondo effect at low temperatures. Devices fabricated from  $\text{GdCl}_3$ @MWNTs exhibit Kondo behavior in the Fermi liquid formalism and non zero bias anomalies very similar to the quantum dot Kondo formalism. The bundled magnetic nanoparticle filled CNT devices represent a system of a multiple quantum conductors with magnetic impurities embedded inside, which is a many body problem. The variables are the magnetic states of the impurities, their multiplicity in a bundle, the spin polarization, symmetry in the conduction channels, hence a very complicated system. The highlight of this study is that even with all these uncertainties, the elusive Kondo effect is observed in a less complicated device configuration. Further work will have to be done to solve the variables highlighted; probably the non zero resonances can be resolved. This study highlights the potential of carbon based spintronic devices fabricated from MWNTs filled with magnetic nanoparticles, an avenue that has not yet been investigated in conventional spintronic research.

#### ACKNOWLEDGMENTS

The support of the CSIR NLC and NRF (SA) towards this research is hereby acknowledged. A.M.S. is thankful to NRF (93549) and the URC/FRC of UJ for financial support.

<sup>1</sup>K. J. Franke, G. Schulze, and J. I. Pascual, *Science* **332**, 940 (2011).

<sup>2</sup>A. Allerdt and A. E. Feiguin, *Phys. Rev. B* **95**, 104402 (2017).

<sup>3</sup>D. Ciudad, Z. C. We, A. T. Hindmarch, E. Negusse, D. A. Arena, X. F. Han, and C. H. Marrows, *Phys. Rev. B* **85**, 214408 (2012).

<sup>4</sup>L. Kouwenhoven and L. Glazman, *Phys. World* **14**, 33 (2001).

<sup>5</sup>G. Falci, D. Feinberg, and F. W. J. Hekking, *Europhys. Lett.* **54**, 255 (2001).

<sup>6</sup>J. Barański and T. Domański, *Phys. Rev. B* **84**, 195424 (2011).

<sup>7</sup>R. Žitko, J. S. Lim, R. López, and R. Aguado, *Phys. Rev. B* **91**, 045441 (2015).

- <sup>8</sup>A. Mugarza, C. Krull, R. Robles, and S. Stepanow, *Nat. Commun.* **2**, 490 (2011).
- <sup>9</sup>F. Kuemmeth, H. O. H. Churchill, P. K. Herring, and C. M. Marcus, *Mater. Today* **13**, 18 (2010).
- <sup>10</sup>L. E. Hueso, J. M. Pruneda, V. Ferrari, G. Burnell, J. P. Valdés Herrera, B. D. Simons, P. B. Littlewood, E. Artacho, A. Fert, and N. D. Mathur, *Nature* **445**, 410 (2007).
- <sup>11</sup>A. R. Rocha, V. M. Garcia Suarez, and S. W. Bailey, *Nat. Mater.* **4**, 335 (2005).
- <sup>12</sup>I. Marangon, C. Ménard Moyon, J. Kolosnjaj Tabi, M. L. Béoutis, L. Lartigue, D. Alloyeau, E. Pach, B. Ballesteros, G. Autret, T. Ninjbadgar, D. F. Brougham, A. Bianco, and F. Gazeau, *Adv. Funct. Mater.* **24**, 7173 (2014).
- <sup>13</sup>M. Urdampilleta, S. Klyatskaya, J. P. Cleuziou, M. Ruben, and W. Wernsdorfer, *Nat. Mater.* **10**, 502 (2011).
- <sup>14</sup>R. Kumari, A. Singh, B. S. Yadav, D. R. Mohapatra, A. Ghosh, P. Guha, P. V. Satyam, M. K. Singh, and P. K. Tyagi, *Carbon* **119**, 464 (2017).
- <sup>15</sup>C. Meyer, C. Morgan, and C. M. Schneider, *Phys. Status Solidi Basic Res.* **248**, 2680 (2011).
- <sup>16</sup>K. Tsukagoshi, B. W. Alphenaar, and H. Ago, *Nature* **401**, 572 (1999).
- <sup>17</sup>R. Thamankar, S. Niyogi, B. Y. Yoo, Y. W. Rheem, N. V. Myung, R. C. Haddon, and R. K. Kawakamia, *Appl. Phys. Lett.* **89**, 033119 (2006).
- <sup>18</sup>P. J. Herrero, J. Kong, H. S. J. van der Zant, C. Dekker, L. P. Kouwenhoven, and S. De Franceschi, *Nature* **434**, 484 (2005).
- <sup>19</sup>T. Inoshita, *Science* **281**, 526 (1998).
- <sup>20</sup>L. Liu, K. Yang, Y. Jiang, B. Song, W. Xiao, L. Li, H. Zhou, Y. Wang, S. Du, M. Ouyang, W. A. Hofer, A. H. C. Neto, and H. J. Gao, *Sci. Rep.* **3**, 1210 (2013).
- <sup>21</sup>S. Xiang, S. Xiao, K. Fujii, K. Shibuya, T. Endo, N. Yumoto, T. Morimoto, N. Aoki, J. P. Bird, and Y. Ochiai, *J. Phys.: Condens. Matter.* **26**, 125304 (2014).
- <sup>22</sup>T. W. Odom, J. L. Huang, C. L. Cheung, and C. M. Lieber, *Science* **290**, 1549 (2000).
- <sup>23</sup>C. Xu, J. Sloan, G. Brown, S. Bailey, V. C. Williams, S. Friedrichs, K. S. Coleman, E. Flahaut, J. L. Hutchison, R. E. Dunin Borkowski, and M. L. H. Green, *Chem. Commun.* **0**, 2427 (2000).
- <sup>24</sup>F. Tuinstra and J. L. Koenig, *J. Chem. Phys.* **53**, 1126 (1970).
- <sup>25</sup>U. Weissker, S. Hampel, A. Leonhardt, and B. Buchner, *Materials* **3**, 4387 (2010).
- <sup>26</sup>M. V. Kharlamova, L. V. Yashina, A. A. Eliseev, A. A. Volykhov, V. S. Neudachina, M. M. Brzhezinskaya, T. S. Zyubina, A. V. Lukashin, and Y. D. Tretyakov, *Phys. Status Solidi B* **249**(12), 2328 (2012).
- <sup>27</sup>M. S. Dresselhaus, A. Jorio, M. Hofmann, G. Dresselhaus, and R. Saito, *Nano Lett.* **10**, 751 (2010).
- <sup>28</sup>X. Zhao, Y. Ando, L. C. Qin, H. Kataura, Y. Maniwa, and R. Saito, *Phys. B: Cond. Mat.* **323**, 265 (2002).
- <sup>29</sup>T. Bortolamiol, P. Lukanov, A. M. Galibert, B. Soula, P. Lonchambon, L. Datas, and E. Flahaut, *Carbon* **78**, 79 (2014).
- <sup>30</sup>A. Jaiswal, R. Das, K. Vivekanand, T. Maity, P. M. Abraham, S. Adyanthaya, and P. Poddar, *J. Appl. Phys.* **107**, 013912 (2010).
- <sup>31</sup>I. D. Zakir'yanova, A. B. Salyulev, and V. A. Khokhlov, *Russ. Metall.* **2011**, 754.
- <sup>32</sup>J. F. Daniel, W. R. Wilmarth, G. M. Begun, and J. R. Peterson, *J. Crystallogr. Spectrosc. Res.* **19**, 39 (1989).
- <sup>33</sup>A. A. Ovchinnikov and V. V. Atrazhev, *Phys. Solid State* **40**, 1769 (1998).
- <sup>34</sup>A. Quetz, I. Dubenko, T. Samanta, H. Vinson, S. Talapatra, N. Ali, and S. Stadler, *J. Appl. Phys.* **113**, 17B512 (2013).
- <sup>35</sup>P. Nozières, *J. Low Temp. Phys.* **17**, 31 (1974).
- <sup>36</sup>J. H. Chen, L. Li, W. G. Cullen, E. D. Williams, and M. S. Fuhrer, *Nature Phys.* **7**, 535 (2011).
- <sup>37</sup>R. McIntosh and S. Bhattacharyya, *Rapid Res. Lett.* **6**(2), 56–58 (2012).
- <sup>38</sup>J. Paaske, A. Rosch, P. Wölfle, N. Mason, C. M. Marcus, and J. Nygård, *Nature Phys.* **2**, 460 (2006).
- <sup>39</sup>K. J. Dempsey, A. T. Hindmarch, H. X. Wei, Q. H. Qin, Z. C. Wen, W. X. Wang, G. Vallejo Fernandez, D. A. Arena, X. F. Han, and C. H. Marrows, *Phys. Rev. B* **82**, 214415 (2010).
- <sup>40</sup>A. Crippa, M. L. V. Tagliaferri, D. Rotta, M. De Michielis, G. Mazzeo, M. Fanciulli, R. Wacquez, M. Vinet, and E. Prati, *Phys. Rev. B* **92**, 035424 (2015).
- <sup>41</sup>J. T. Lee, D. H. Chae, Z. Yao, and J. Sessler, *Chem. Commun.* **48**, 4420 (2012).